

Core Design and Optimization for Better Misalignment Tolerance and Higher Range of Wireless Charging of PHEV

Mostak Mohammad, *Student Member, IEEE*, Seungdeog Choi, *Senior Member, IEEE*,
Md Zakirul Islam, *Student Member, IEEE*, Sangshin Kwak, *Member, IEEE*,
and Jeihoon Baek, *Member, IEEE*

Abstract—In this paper, a design and optimization method of ferrite core is proposed for wireless charging system of plug-in hybrid electric vehicle to improve its misalignment tolerance and minimize the core loss. While optimizing for higher misalignment tolerance, the primary focus is given to maintain uniform flux density in the core to minimize the core loss. An excessive use of core increases the weight and loss of the system, which need to be minimized through optimal design. Moreover, the flux density changes with misalignment, and the misalignment probability for car parking could be different in different direction. Hence the directional probability of misalignment needs to be considered during core design. In this paper, a core structure is proposed for a circular and bar-shaped core to achieve uniform flux density and an optimization method is proposed based on sequential nonlinear programming algorithm in FEA. Compared to typical uniform thickness core structure, in an optimized core, the core loss per unit volume is reduced by 30% for circular core and by 39% for bar-shaped core and the core volume per unit core loss is reduced by 17.5% in optimized circular shaped core.

Index Terms—Ferrite core, inductive charging, lateral misalignment, magnetic coupling, transportation, wireless power transfer.

I. INTRODUCTION

BOTH the low and high power wireless charging systems are being extensively investigated for last two decades. Medium power inductive wireless charging is getting more matured for EV and plug-in hybrid electric vehicle (PHEV) charging, and prediction indicates that this wireless charger market will expand to \$4.6 billion by 2019 [1]. In commonly used contact-less charging application, the transmitter is placed on the floor and the receiver is mounted at the bottom of the

Manuscript received August 17, 2016; revised December 4, 2016; accepted January 15, 2017. Date of publication February 2, 2017; date of current version June 14, 2017. This work was supported in part by the UA NSF I-Corps Sites Program funded by the National Science Foundation, USA, under Grant CNS-1322061 and in part by the National Research Foundation of Korea, Korea Government, under Grant 2014R1A2A2A01006684.

M. Mohammad, S. Choi, and M. Z. Islam are with the Electrical and Computer Engineering Department, University of Akron, Akron, OH 44325 USA (e-mail: mm251@zips.uakron.edu; schoi@uakron.edu; mi15@zips.uakron.edu).

S. Kwak is with the Electrical and Electronics Engineering Department, Chung-Ang University, Seoul 156756, South Korea (e-mail: sskwak@cau.ac.kr).

J. Baek is with the High Speed Railway System Development, Korea Railroad Research Institute, Uiwang 437825, South Korea (e-mail: jhbaek@gmail.com).

Digital Object Identifier 10.1109/TTE.2017.2663662

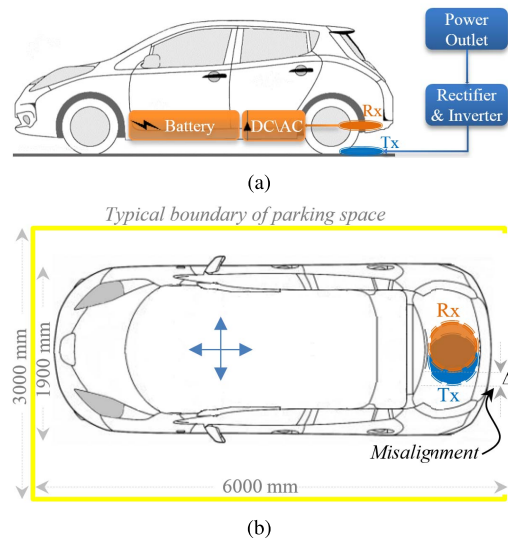


Fig. 1. (a) Basic components and (b) typical misalignment of wireless charging system for EV application.

vehicle as shown in Fig. 1(a). As the vehicle is parked, it is usual that there will be a certain level of misalignment between that transmitter and receiver. The application of wireless power in PHEV is more challenging because of this unpredictable car parking, which causes mainly the horizontal misalignment as shown in Fig. 1(b). For a typical car parking on a flat parking area, the horizontal misalignment is more likely to happen than angular or vertical misalignment, therefore, the system requires to be designed such that it becomes more tolerant to the horizontal misalignment. It takes 8–17 h for Level 1 (120 VAC at 12–16A) and level 2 (240 VAC at 15–80A) charging system to fully charge a 24kWh EV battery. Therefore stability and high efficiency is essential, and drop of efficiency due to misalignment is not practically tolerable. Strong coupling between the high-quality transmitter (Tx) and receiver(Rx) coils can enhance the misalignment tolerance and range of operation.

In a typical wireless charging system, two electrically isolated coils, tuned at same resonant frequency, are magnetically coupled to effectively transmit power over a few millimeters to several hundred millimeters. This distance depends on the

size of the coils, the magnetic coupling between them and the operating frequency [2]. As the distance between the transmitter and the receiver increases, the magnetic coupling can be critically low to sustain efficient power transfer. Therefore under the practical limitation of coil size and operating frequency, the wireless power transfer is challenging for a large gap between Tx–Rx. The system gets even more susceptible to parametric fluctuation and low efficiency under the horizontal and angular misalignment [3].

High permeability ferrite core can enhance the misalignment tolerances of this high power wireless charging within certain limit of misalignment. Different core shapes are proposed in the previous literature to maximize the coupling coefficient using ferrite plate and ferrite bar, interturn core, EE-type, and CC-type core [4]–[14]. An excessive investigation on core design is done in [15] and [16], where the characteristics of bar or block shaped core with different arrangement and configuration are shown and an optimization approach is proposed. But the bar shaped core with uniform thickness cannot provide the maximum core utilization. In [5], [17], [18], wireless charging system with planar coil and ferrite core has been proposed in its simplest form, which do not provide the optimum configuration of the core, especially considering the vehicular application. To make the system more misalignment insensitive, array of inductor is proposed in [19], which although increases the misalignment tolerance, but it significantly reduces the range of vertical gap between Tx and Rx, therefore not feasible for HEV application where the airgap is comparatively large. A cylindrical core for helical transmitter coil is shown in [20] to improve the flux linkage capability and transmission efficiency. But the cylindrical coil increases the height of the Tx and it uses large amount of core, and therefore, not suitable for vehicular charging system. For PHEV charging, the Tx and Rx have to be highly efficient as well as comfortably small and of minimum weight. Therefore, planar coil is best suitable with planar core and shield. A core on the receiver side will increase the weight, which needs a serious consideration of optimization. Again, significant core loss would incur with the introduction of the core, especially at high current and high operating frequency. Therefore, an optimization approach for core design is critically important considering core loss, size, and weight.

From the safety and regulation standpoint, one of the main purposes of using ferrite core and conductor shield is to control the magnetic and electromagnetic emission around the charging system. This emission depends on the Tx–Rx topology, size, coupling coefficient, and misalignment as well [21], [22]. Therefore, it also needs to be considered in the core design and optimization process.

The optimization of ferrite core for wireless charging in PHEV had been investigated for different core shapes and orientations [23]. The main focus of that work was to maximize the misalignment tolerance using uniformly thick ferrite bars. While the misalignment tolerance was enhanced significantly, the core loss minimization had not been addressed thoroughly. In this paper, in addition to enhancing the coupling coefficient, the core thickness is also considered to minimize the core loss. A new core structure and an optimization method are proposed

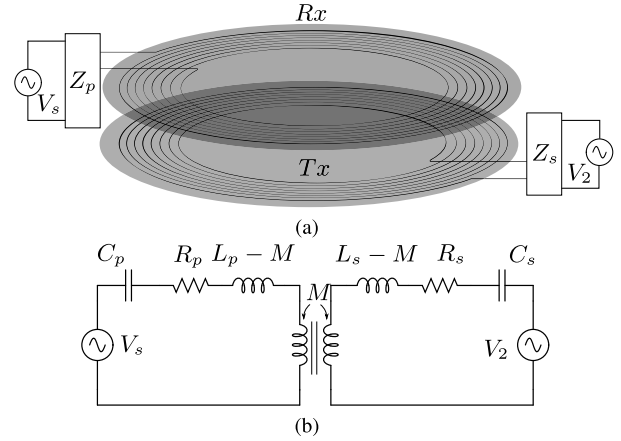


Fig. 2. (a) Basic resonant coil pair for WPT. (b) Equivalent circuit for series-series compensated system.

to enhance the magnetic coupling and minimize the core loss under the weight constraint. The minimization of core loss and weight are investigated under different alignment between transmitter and receiver.

II. CORE EFFECT ON WIRELESS CHARGING

Inductive power transfer is one of the most popular near-field wireless power transfer methods. It is highly efficient for limited distances and strong magnetic coupling, and therefore, it has been adopted for this medium power automotive application. Fig. 2(a) shows the transmitter and receiver of a typical planar circular wireless charging system, where two magnetically coupled coils are isolated by 100 to 200 mm airgap for vehicular application. The size of the Tx and Rx can be different for different vehicle size, battery capacity, and misalignment pattern.

When the two coils are tuned by the matching impedance Z_p and Z_s to operate at same resonant frequency, power can be transferred efficiently between them. The maximum power transfer efficiency η_{\max} at an optimum load impedance $Z_{L_{\max}}$ for a series-series compensated core-less wireless charging system can be expressed as [24]

$$\eta_{\max} = \frac{1}{1 + \frac{2}{k\sqrt{Q_p Q_s}}} \quad (1)$$

where Q_p and Q_s are the unloaded quality factor of the compensated transmitter and receiver coil and k is the coupling coefficient between them. The quality factors are given as

$$Q_p = \frac{\omega L_p}{R_p}, \quad Q_s = \frac{\omega L_s}{R_s} \quad (2)$$

where R_p and R_s represent the resistances of the primary and secondary coils, consists of dc resistances $R_{p,dc}$, $R_{s,dc}$ and ac resistances $R_{p,ac}$, $R_{s,ac}$. The ac resistance of the air-core system mainly includes the resistances due to traditional proximity effect between neighboring turns and the skin effect of the coil. The incorporation of the ferrite core might increase the resistance of the coil as shown in [23]. The coupling coefficient between the transmitter and the receiver is expressed

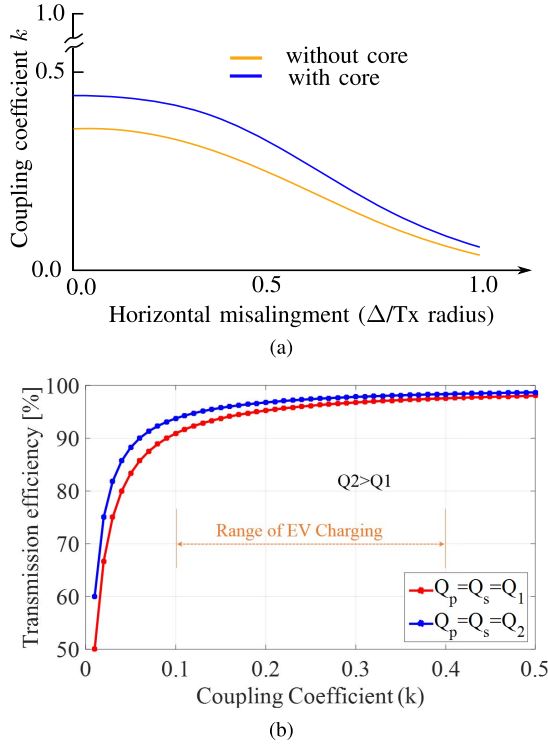


Fig. 3. Variation of (a) coupling coefficient with misalignment and (b) efficiency with coupling coefficient.

as

$$k = \frac{M}{\sqrt{L_p L_s}} \quad (3)$$

where L_p and L_s are the total inductance of Tx and Rx, M is the mutual inductance between them, and ω is the operating frequency.

The maximum achievable power transfer efficiency can be improved by increasing the quality factors and the coupling factor, as given in (1). But Q_p and Q_s depend on the physical constraint of the system. It can be increased by increasing the inductance and operating frequency, and by reducing the parasitic resistance. But, as the number of turn increases, both the inductance and the parasitic resistance increases. Therefore, the inductance cannot be increased arbitrarily. Again, as already mentioned in Section I, the operating frequency ω is limited due to the switching loss of semiconductor switches, and copper and core loss in Tx–Rx. The copper loss can be minimized using appropriate litz wire based on operating frequency and current through transmitter and receiver coil [25]. According to SAE J2954, the switching frequency is decided between 80.38–90 kHz for EV charging system [26], while the current depends on the power rating of the system as well as the compensation topology.

The other parameter in (1) is the coupling coefficient k , which varies significantly with the misalignment as shown in Fig. 3(a). The variation of coupling coefficient, at its lower range, significantly affects the power transmission efficiency. Fig. 3(b) shows the variation of power transfer efficiency against coupling coefficient and signifies its effect at low

coupling coefficient. Therefore, it requires to sustain a minimum value of coupling factor for an acceptable range of misalignment, and it can be done through an optimum core design, especially when the coil size is limited. Fig. 3(a) indicates that the coupling coefficient can be significantly enhanced using core.

This efficiency versus coupling characteristics is critically important for EV charging, as it operate just above the critical coupling factor [27], and therefore, under misalignment the system is highly susceptible to operate with low efficiency.

III. CORE DESIGN FOR WIRELESS CHARGER FOR PHEV

The core partially provides a low reluctance path for the magnetic flux while the rest of its path goes through the airgap. The overall effect of this core in the flux path can be represented as a reduction of reluctance or an enhancement of effective relative permeability of the flux path; therefore, it increases both the self and mutual inductance of the Tx and Rx. However, it introduces the core loss and additional parasitic series resistances, R_{p_core} , R_{s_core} to the transmitter and receiver and consequent losses [23]. All these effects depend on the core material properties, core geometry, and flux distribution and operating frequency. From the core design standpoint, it is required to ensure that, the flux density remains below saturation, as well as uniform, to achieve low loss and better utilization of the core. The flux density at any point in the core, expressed in (4), depends on the current through the coil, coil span and turn number, coil position, and length, thickness and permeability of the core. Most importantly, it also depends on the misalignment between the transmitter and the receiver

$$B_{core}(x, y, z) = f(I_p, I_s, w_{coil}, N_p, N_s, d, \Delta, \mu_r, l_{core}, w_{core}, t_{core}) \quad (4)$$

where

I_p	= current through transmitter coil;
I_s	= current through receiver coil;
w_{coil}	= total width of the coil;
N_p	= number of turn in primary coil;
N_s	= number of turn in secondary coil;
d	= airgap between Tx and Rx;
Δ	= lateral misalignment;
μ_r	= relative permeability of ferrite core;
l_{core}	total length of the core;
w_{core}	width of the discrete core (e.g., bar shaped core); and
t_{core}	= thickness of the core.

The relative permeability of the ferrite core is usually in the range of 1000–5000 and saturation flux density is in the range of 370–570 mT. While those properties of a ferrite core are usually relatively insensitive to temperature and frequency, in many ferrites those properties vary with the temperature and frequency as well [28]. In this analysis the relative permeability of the ferrite core is 2500 and the saturation flux is 370 mT.

Tx and Rx with only two pair of coil provide minimum misalignment tolerance, and also have minimum weight. On the

TABLE I
INITIAL PARAMETERS

Parameter	Initial value
Airgap, d	150mm
Maximum misalignment, δ	300mm
Coil internal radius, r_i	150mm
Coil span, w_{coil}	100mm
Number of turn, N_p, N_s	20, 20
Transmitter current, I_p	20A
Receiver current, I_s	20A
Maximum Tx, Rx diameter (D_{max})	600mm

other hand, core for both transmitter and receiver covering maximum allowed area, provide the maximum misalignment tolerance, but at the same time, it adds large amount of weight to the system. While the optimized core maximizes the misalignment tolerance and minimizes the core loss with an allowed amount of core. The loss of the high power ferrite core for can be expressed as [29]

$$P_{core} = C_m f^\alpha B_{max}^\beta \quad (5)$$

where C_m , α , and β are the constant which depends on the core properties. Low loss power ferrite cores, e.g., TDK PC44, PC47, FDK 6H40, 6H45, are potential candidates for high power wireless charging systems. In this paper, the properties are investigated for a MnZn-family ferrite core FDK 6H40 which has been designed for high power applications of 100–500 kHz frequency range [30]. The coefficients of this core material are $C_m = 2.0312$, $\alpha = 1.418$, and $\beta = 2.755$.

In this paper, the system is designed for a 5 kW wireless charging system for PHEV/EV application, operating at 85 kHz. Both the transmitter and receiver are of the same configurations, where the maximum diameter of the transmitter and receiver is 600 mm and they are separated by 150 mm vertical distance. The optimization process is initiated with the specifications given in Table I. The appropriate selection criteria of litz wire to subdue the skin effect and evenly distribute the high frequency current, based on operating frequency and current through the coil is given in detail in [25]. In this system, both the coils are of planar spiral shape with 20 equally spaced turns, where AWG38x800 litz wire is chosen for its suitability for 20 A, 50–100 kHz. The conductive shield has a significant effect on reducing the leakage field emission, but it also impacts the self and mutual inductance of the Tx–Rx and adds eddy current loss. Throughout the analysis, a 5 mm thick aluminum plate is used as the conductive shield with the same radius as ferrite core. The aluminum shield has reduced the self and mutual inductance of the system by 7%–10%. Both the transmitter and receiver are series compensated and operating at nearly resonant frequency with unity gain; hence I_p and I_s are assumed the same. Depending on the topological variation to series–parallel, parallel–series, and parallel–parallel, the current of the primary and secondary will vary and the design can be extended accordingly. With the similar assumption, the phase difference between the primary

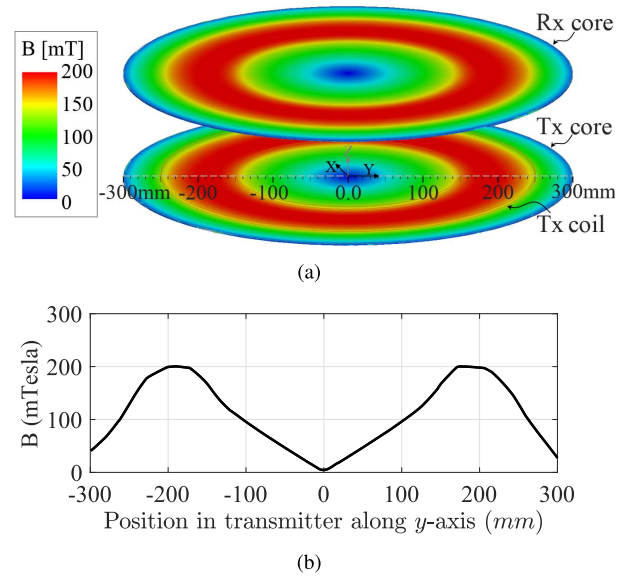


Fig. 4. For a uniform thickness core. (a) Flux density distribution across the Tx and Rx core. (b) Flux density in the transmitter along the y-axis.

and secondary current is considered zero. This assumption yields the highest flux density at any given current; whereas a phase difference between the transmitter and receiver current, the maximum flux density reduces. Although the transmitter and receiver are considered of the same configuration in this paper, their configuration will vary for different applications. In [31], different transmitter and receiver size and coil turn number are investigated for estimating coupling coefficient, k . Due to the generality of the proposed optimization method, it can be extended for those systems accordingly. In this paper, first the proposed method is investigated on a circular core, it is applied for other core configuration to further reduce the weight and loss, through a tradeoff with coupling coefficient.

A. Core Design for Perfectly Aligned Condition

The flux density in a uniformly thick circular core with a planar spiral coil is investigated for the parameters given in Table I for perfectly aligned transmitter and receiver. The significant variation of flux density distribution in uniform thickness transmitter and receiver core is shown in Fig. 4(a). The regions in the core around central and outer edge show very low flux density and low utilization of the core, and the red color regions around the coil of Tx and Rx show comparatively higher flux density, hence higher core loss. This wide nonuniformity of the flux density in a uniform thickness core is more precisely exhibited in Fig. 4(b), which shows the flux density in the transmitter along the y-axis. The flux density at the center of the transmitter core is very low and it increases symmetrically along the radially outward direction until it reaches the maximum flux density near the central turn of the coil. Then, the flux density decreases toward the outer edge of the core. It shows that, in a uniform thickness core a significant part of the core is left underutilized with low flux density.

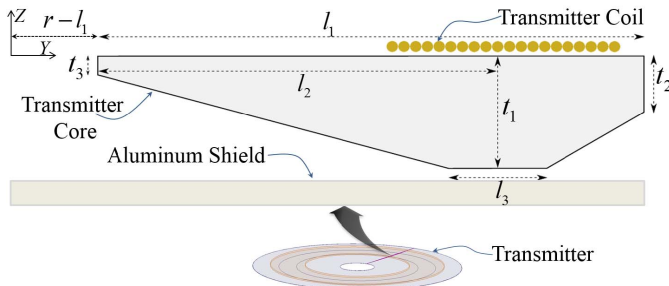


Fig. 5. Radial cross-sectional view of proposed circular core with linearly varying thickness to achieve uniform flux density.

The core loss can be reduced by designing the core structure such that flux density becomes uniform throughout the core. As the flux density is inversely proportional to the core cross-sectional area, hence the core thickness along its radial direction can therefore be optimized for uniform flux density and consequently, core loss reduction. Fig. 4(b) shows that, the flux density in a uniform thickness transmitter varies nonlinearly along the radial direction. Therefore, a core structure with nonlinearly varying thickness would give highly uniform flux density and least core loss. But design and optimization complexity, and the cost of fabrication would increase significantly for a core having nonlinearly varying thickness. Therefore, for the simplicity and generality of core structure and optimization process, a core shape is proposed consisting of several sections of linearly varying thickness. Based on the flux density variation, the number of sections for the optimization process can be varied accordingly.

Following the flux density in the uniform thickness core, the proposed core shape to optimize for circular core is given in Fig. 5, where all the length (l) and thickness (t) are to be optimized through finite element analysis (FEA) analysis. The sequential nonlinear programming algorithm is adopted to optimize these parameters to achieve uniform flux density throughout the core.

At the center area of the transmitter and receiver, there is put no core, as the flux density is very low till $y = r - l_1$, where r is the radius of the transmitter. From $r - l_1$ to r the core thickness is varied according to Fig. 5, to make the flux density uniform around 150 mT. The resultant flux density is found mostly in the range of 130–150 mT, which can be made even more uniform using more number of sections with linearly varying thickness or designing a more complex structure with nonlinearly varying thickness. In this paper, a simple structure is chosen with three linearly varying slopes, which provided the ease of parametric representation as well as freedom of optimization.

The optimized parameter of the core to achieve the targeted uniform flux density 150 mT is given in Table II. Compared to the largely varying flux density distribution in the uniform thickness core in Fig. 4(a), the flux density distribution in the optimized transmitter and receiver core shows much higher uniformity, which is shown in Fig. 6(a). More details of the flux density profile in the transmitter core are shown in Fig. 6(b).

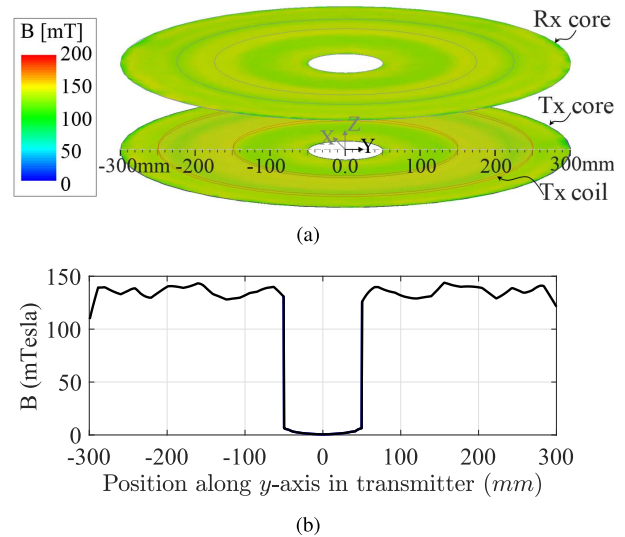


Fig. 6. For optimized thickness core. (a) Flux density distribution in transmitter and receiver. (b) Flux density in the transmitter along the y-axis.

TABLE II
OPTIMIZED PARAMETERS FOR CIRCULAR CORE

Parameter	Optimized value
Maximum core thickness, t_1	3.2mm
Inside edge core thickness, t_3	0.5mm
Outer edge core thickness, t_2	0.7mm
Core length, l_1, l_2, l_3	250mm, 200mm, 50mm
Maximum flux density, B_{max}	150mT

B. Core Design Considerations for Misalignment

Although this optimized structure provides the maximum core utilization, it has limitations for the application where misalignment is a common phenomenon. At different misalignment conditions, the flux density pattern changes in the core. Under horizontal misalignment Δ , the flux density distribution calculated in FEA for a uniform thickness core plate, is shown in Fig. 7(a). Fig. 7(b) and (c) shows that the maximum flux density occurs at the same position as before, but under misalignment an asymmetry occurs between those peaks and the flux density increases in the central area of the core, compared to alignment condition. The portion of core that shifts outside the common area shows increased flux density as the leakage flux increases in those areas. Fig. 7 also shows the change in flux density for the variation of normalized misalignment, $\Delta/(r_{max})$ from 0% to 75%.

It shows that, the flux density at the inner edge of the core increases significantly, compared to other parts. Simply following the optimization method and increasing only t_3 to adjust this high flux density would require large amount of core as shown in Fig. 8. Rather, a close inspection on the flux density for this new core structure, shown in Fig. 9, gives an indication that a circular ring of core at its inner edge can reduce this misalignment induced high flux density through minimum amount of additional core. The cross-sectional view of the optimized core with the inner ring and the resultant flux density is shown in Fig. 10.

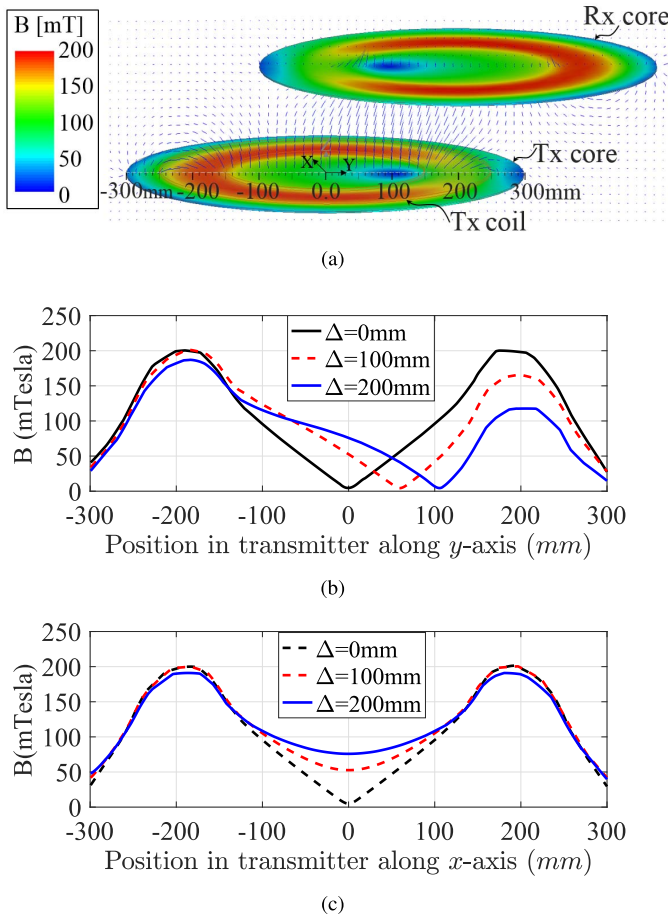


Fig. 7. Uniform thickness core under misalignment. (a) Flux density distribution in Tx and Rx. (b) Flux density along x-axis and (c) y-axis.

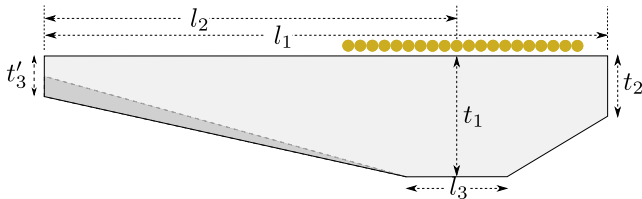


Fig. 8. Cross section of proposed optimized core considering horizontal misalignment.

The relation between core loss and frequency is given in (5). It shows that at the same flux density, the total core loss will increase significantly with frequency. At different frequency, the comparison of core loss between the core with uniform thickness and uniform flux density configurations is shown in Fig. 11(a), where approximately 30% core loss is reduces in uniform flux density core configuration.

C. Optimization With Bar Core

The core loss and weight can be further reduced through a tradeoff with slight reduction of coupling coefficient. Again, weight is a critical factor for vehicle charging application, especially for the receiver, as it is directly mounted at the bottom of the vehicle. As ferrite is a heavy material, when included in the design of the core, the total amount of material

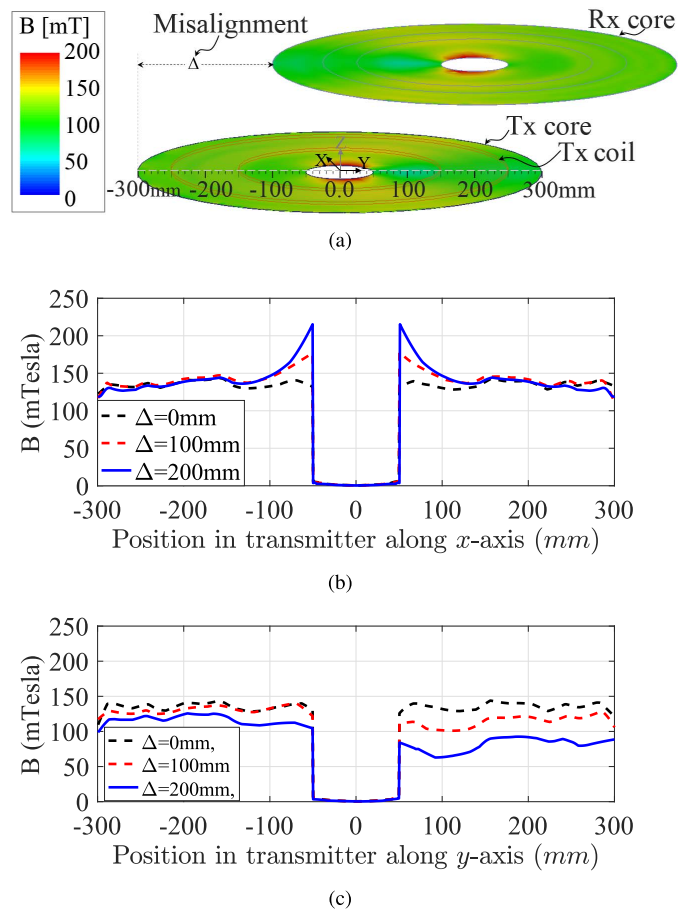


Fig. 9. For the optimized core given in Fig. 8. (a) Flux density distribution in Tx and Rx. (b) Flux density along x-axis and (c) y-axis, for different misalignment conditions.

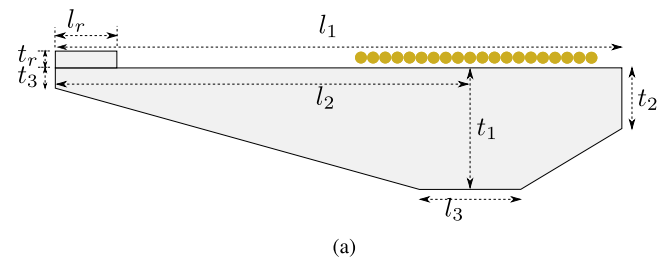
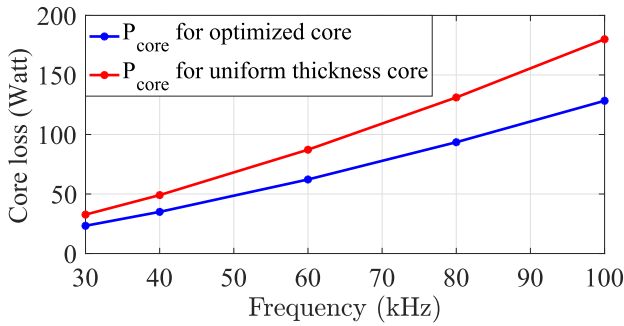
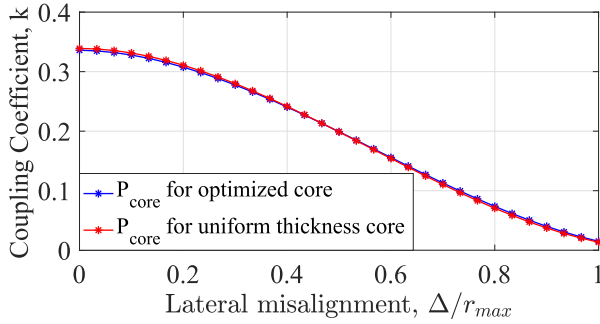


Fig. 10. Optimized core. (a) Cross section showing inner ring to adapt with misalignment. (b) Flux density distribution under 200 mm lateral misalignment.

used in the receiver would require to be minimized even more. Therefore, the objectives of the core optimization are as follows:



(a)



(b)

Fig. 11. Comparison of (a) core loss and (b) coupling coefficient between uniform flux and uniform thickness core configurations designed for 20 A current.

- 1) minimization of core loss;
- 2) minimization of total core weight;
- 3) maximization of coupling factor and misalignment tolerance.

An objective function Φ is proposed in (6) to reduce the core loss and weight, while maximizing the magnetic coupling and efficiency under certain constraint of weight and efficiency

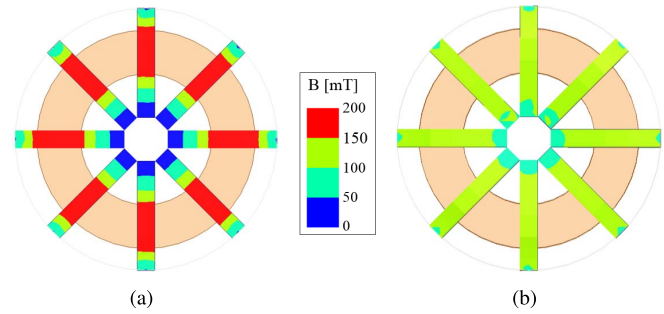
$$\Phi^2 = c_1 \left(\frac{P_{core}}{P_{core,ref}} \right)^2 + c_2 \left(\frac{W_{core}}{W_{core,ref}} \right)^2 + c_3 \left(\frac{k_{ref}}{k} \right)^2 \quad (6)$$

where

Φ	= Objective Function;
P_{core}	= hysteresis loss in core;
$P_{core,ref}$	= hysteresis loss in reference core;
W_{core}	= total core weight;
$W_{core,ref}$	= total weight of reference core;
k	= magnetic coupling factor;
k_{ref}	= magnetic coupling factor with reference core.

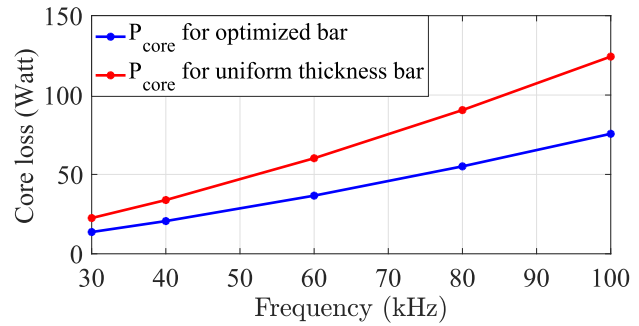
and, c_1, c_2, c_3 are the weighting factor for core loss, weight, and magnetic coupling factor correspondingly; these will depend on the design specifications, and requirement and limitation of the system. And all the reference values are taken from initially optimized system shown in Fig. 10(a).

The ferrite material has high resistivity which reduces the eddy current loss, and the high flux density at high frequency increases the hysteresis loss. Therefore, the eddy current loss in the core is ignored and the calculated core loss is the hysteresis loss. This core loss is dependent on the properties



(a)

(b)



(c)

Fig. 12. Flux density distribution in (a) uniform thickness core, (b) optimized core, and (c) their core loss comparison.

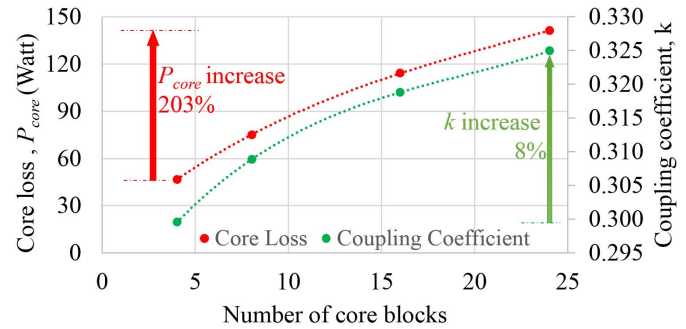


Fig. 13. Variation of core loss and coupling coefficient with segregation of the same amount of core.

of core material, magnetic flux density in the core and the operating frequency as expressed in (5).

The uniform thickness bar shaped core is the most widely used configuration for midpower wireless charging system. But the uniform thickness bar shaped core suffers due to low utilization like the uniform thickness circular plate core. Fig. 12 shows the flux density in uniform thickness bar core. As the provided configuration is symmetric around the z -axis, the previous optimization method can be applied to get the thickness profile of the bar for uniform flux density in the core along the y -axis direction. Fig. 12(c) shows the loss comparison of the uniform thickness bar core and uniform flux bar core for different frequency; it shows that approximately 39.2% core loss is reduced in the optimized bar.

If the same amount of core is used, segregated into increased number of equally spaced blocks with reduced width, the self-inductance, mutual inductance, and coupling

TABLE III
COMPARATIVE DATA OF DIFFERENT CORE CONFIGURATION

Parameter	Uniform thickness circular core	Optimized circular core	Optimized bar core (shown in Fig. 14)
Coupling coefficient (at $\Delta = 0$), k	0.330	0.303	0.298
Core volume, (cm^3)	1200	1200	704
Core loss at 80kHz, P_{core} (W)	131.1	93.0	44.1

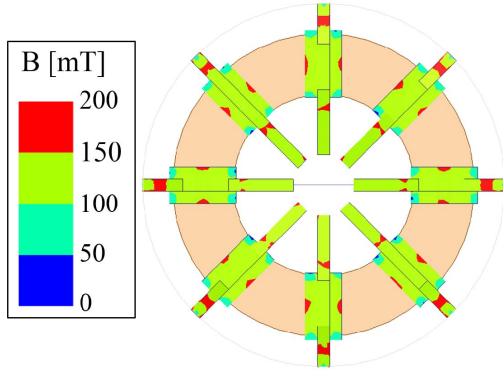


Fig. 14. Optimized core structure with maximum utilization and lowest core loss.

coefficient increases. But at the same time, the core loss also increases significantly as shown in Fig. 13. Therefore, depending on the value of prioritizing design parameter c_1 , c_2 , c_3 the optimized core will be different.

Fig. 12(b) also depicts that, although the flux density is uniform outward, the core utilization is still low around inner edge of the core, and it cannot be made any thinner due to mechanical stability. But the inside width of the core can be reduced, and thereby, better core utilization can be achieved. A new more optimized core configuration is given in Fig. 14, which gives lower loss and weight at the same coupling coefficient. The comparative data of core volume, core loss and coupling coefficient are given in Table III. The core utilization can be further enhanced using more complex shaped bar core, but that will increase the design complexity and manufacturing cost.

IV. CONCLUSION

In this paper, a core design and optimization method is given to minimize loss, and weight, and maximize coupling coefficient of a wireless charger for electric vehicle. It is found that, compared to uniform thickness core, the core loss per unit volume can be reduced by 30% for a circular core configuration; flux density is maintained uniform in the core. Again, the effect of misalignment on flux density in the core and the required modification in the design is shown using minimum additional core. Compared to circular core, bar shaped discrete core allows to further reduce the weight and loss through a tradeoff with coupling coefficient. To reduce the loss, the bar shaped core needs to be kept tightly accumulated near the direction of higher misalignment probability. While the loss and weight is reduced in the

bar shaped core, it increases the thickness of core, hence the volume of the pad. Finally, the optimization approach shows the variation of core configuration for varying priorities among reduction of core loss, and weight and enhancement of coupling coefficient. In the future research, the fringe field emission will be incorporated as constraints in the ferrite core and conductive shield design and optimization algorithm.

REFERENCES

- [1] Acute Market Reports. *Wireless Car Charging: Market Shares, Strategies, and Forecasts, Worldwide, 2013 to 2019*, May 1, 2016. [Online]. Available: <http://www.acutemarketreports.com>
- [2] C. Zheng, H. Ma, J.-S. Lai, and L. Zhang, "Design considerations to reduce gap variation and misalignment effects for the inductive power transfer system," *IEEE Trans. Power Electron.*, vol. 30, no. 11, pp. 6108–6119, Nov. 2015.
- [3] B. W. Flynn and K. Fotopoulou, "Rectifying loose coils: Wireless power transfer in loosely coupled inductive links with lateral and angular misalignment," *IEEE Microw. Mag.*, vol. 14, no. 2, pp. 48–54, Mar. 2013.
- [4] H. Kim *et al.*, "Coil design and measurements of automotive magnetic resonant wireless charging system for high-efficiency and low magnetic field leakage," *IEEE Trans. Microw. Theory Techn.*, vol. 64, no. 2, pp. 383–400, Feb. 2016.
- [5] S. Santalunai, C. Thongsopa, and T. Thosdeekoraphat, "An increasing the power transmission efficiency of flat spiral coils by using ferrite materials for wireless power transfer applications," in *Proc. 11th Int. Conf. Elect. Eng./Electron., Comput., Telecommun. Inf. Technol. (ECTI-CON)*, May 2014, pp. 1–4.
- [6] C.-C. Hou, Y.-H. Teng, W.-P. Chang, and K.-Y. Chang, "Analysis and comparison of EE-type and CC-type cores for wireless power transfer systems," in *Proc. 9th Int. Conf. Power Electron., ECCE Asia (ICPE-ECCE Asia)*, Jun. 2015, pp. 1950–1954.
- [7] T. C. Y. Ho, B. Gomersall, and L. Ran, "Contactless charging for electric vehicles with a large air gap," in *Proc. 14th Eur. Conf. Power Electron. Appl. (EPE)*, Aug./Sep. 2011, pp. 1–10.
- [8] T. Maruyama, K. Yamamoto, S. Kitazawa, K. Kondo, and T. Kashiwagi, "A study on the design method of the light weight coils for a high power contactless power transfer systems," in *Proc. 15th Int. Conf. Elect. Mach. Syst. (ICEMS)*, Oct. 2012, pp. 1–6.
- [9] M. Chigira, Y. Nagatsuka, Y. Kaneko, S. Abe, T. Yasuda, and A. Suzuki, "Small-size light-weight transformer with new core structure for contactless electric vehicle power transfer system," in *Proc. IEEE Energy Convers. Congr. Expo.*, Sep. 2011, pp. 260–266.
- [10] K. Aditya and S. S. Williamson, "Design considerations for loosely coupled inductive power transfer (IPT) system for electric vehicle battery charging—A comprehensive review," in *Proc. IEEE Transp. Electrification Conf. Expo (ITEC)*, Jun. 2014, pp. 1–6.
- [11] S. Y. Choi, B. W. Gu, S. Y. Jeong, and C. T. Rim, "Advances in wireless power transfer systems for roadway-powered electric vehicles," *IEEE Trans. Emerg. Sel. Topics Power Electron.*, vol. 3, no. 1, pp. 18–36, Mar. 2015.
- [12] C. Park, S. Lee, S. Y. Jeong, G.-H. Cho, and C. T. Rim, "Uniform power I-type inductive power transfer system with DQ-power supply rails for on-line electric vehicles," *IEEE Trans. Power Electron.*, vol. 30, no. 11, pp. 6446–6455, Nov. 2015.
- [13] Y. H. Sohn, B. H. Choi, E. S. Lee, and C. T. Rim, "Comparisons of magnetic field shaping methods for ubiquitous wireless power transfer," in *Proc. IEEE PELS Workshop Emerg. Technol., Wireless Power (WoW)*, Jun. 2015, pp. 1–6.

- [14] Y. Tang, F. Zhu, Y. Wang, and H. Ma, "Design and optimizations of solenoid magnetic structure for inductive power transfer in EV applications," in *Proc. 41st Annu. Conf. IEEE Ind. Electron. Soc. (IECON)*, Nov. 2015, pp. 001459–001464.
- [15] M. Budhia, G. A. Covic, and J. T. Boys, "Design and optimization of circular magnetic structures for lumped inductive power transfer systems," *IEEE Trans. Power Electron.*, vol. 26, no. 11, pp. 3096–3108, Nov. 2011.
- [16] A. Zaheer, M. Budhia, D. Kacprzak, and G. A. Covic, "Magnetic design of a 300 W under-floor contactless power transfer system," in *Proc. 37th Annu. Conf. IEEE Ind. Electron. Soc. (IECON)*, Nov. 2011, pp. 1408–1413.
- [17] T. Diekhans and R. W. D. Doncker, "A dual-side controlled inductive power transfer system optimized for large coupling factor variations and partial load," *IEEE Trans. Power Electron.*, vol. 30, no. 11, pp. 6320–6328, Nov. 2015.
- [18] O. H. Stielau and G. A. Covic, "Design of loosely coupled inductive power transfer systems," in *Proc. Int. Conf. Power Syst. Technol. (PowerCon)*, vol. 1, 2000, pp. 85–90.
- [19] H. R. Ahn, M. S. Kim, and Y. J. Kim, "Inductor array for minimising transfer efficiency decrease of wireless power transmission components at misalignment," *Electron. Lett.*, vol. 50, no. 5, pp. 393–394, Feb. 2014.
- [20] W. Ding and X. Wang, "Magnetically coupled resonant using Mn-Zn ferrite for wireless power transfer," in *Proc. 15th Int. Conf. Electron. Packag. Technol. (ICEPT)*, Aug. 2014, pp. 1561–1564.
- [21] F. Y. Lin, G. A. Covic, and J. T. Boys, "Leakage flux control of mismatched IPT systems," *IEEE Trans. Transport. Electrific.*, to be published.
- [22] J. M. Miller, O. C. Onar, and M. Chinthavali, "Primary-side power flow control of wireless power transfer for electric vehicle charging," *IEEE J. Emerg. Sel. Topics Power Electron.*, vol. 3, no. 1, pp. 147–162, Mar. 2015.
- [23] M. Mohammad, S. Kwak, and S. Choi, "Core design for better misalignment tolerance and higher range of wireless charging for HEV," in *Proc. IEEE Appl. Power Electron. Conf. Expo. (APEC)*, Mar. 2016, pp. 1748–1755.
- [24] H. Takanashi, Y. Sato, Y. Kaneko, S. Abe, and T. Yasuda, "A large air gap 3 kW wireless power transfer system for electric vehicles," in *Proc. IEEE Energy Convers. Congr. Expo. (ECCE)*, Sep. 2012, pp. 269–274.
- [25] J. M. Miller and A. Daga, "Elements of wireless power transfer essential to high power charging of heavy duty vehicles," *IEEE Trans. Transport. Electrific.*, vol. 1, no. 1, pp. 26–39, Jun. 2015.
- [26] SAE J2954. *Task Force on Wireless Power Charging*, accessed on Jan. 30, 2016. [Online]. Available: <http://www.sae.org>
- [27] A. P. Sample, D. T. Meyer, and J. R. Smith, "Analysis, experimental results, and range adaptation of magnetically coupled resonators for wireless power transfer," *IEEE Trans. Ind. Electron.*, vol. 58, no. 2, pp. 544–554, Feb. 2011. [Online]. Available: <https://www.mag-inc.com>.
- [28] (2013). *Soft Ferrites and Accessories, Data Handbook*. [Online]. Available: <http://www.ferroxcube.com>
- [29] J. Mühlethale, J. Biela, J. W. Kolar, and A. Ecklebe, "Core losses under the DC bias condition based on Steinmetz parameters," *IEEE Trans. Power Electron.*, vol. 27, no. 2, pp. 953–963, Feb. 2012.
- [30] FDK Corporation. *Development of a Ferrite Material for Inductive Chargers*, accessed on Nov. 25, 2016. [Online]. Available: <http://www.fdk.com>
- [31] F. Y. Lin, C. Carretero, G. Covic, and J. Boys, "Reduced order modelling of the coupling factor for varying sized pads used in wireless power transfer," *IEEE Trans. Transport. Electrific.*, to be published.



Mostak Mohammad (S'15) received the B.Sc. degree in electrical and electronic engineering from the Bangladesh University of Engineering and Technology, Dhaka, Bangladesh, in 2009. He is currently pursuing the Ph.D. degree in power program with the University of Akron, Akron, OH, USA, in 2014.

From 2009 to 2014, he was a Radio Network Planner with Robi Axiata Limited, Dhaka. His current research interests include wireless charging system for electric vehicles, high frequency resonant power converter, and application of widebandgap devices.



Seungdeog Choi (S'07–M'12–SM'16) received the B.S. degree from Chung-Ang University, Seoul, South Korea, in 2004, the M.S. degree from Seoul National University, Seoul, in 2006, and the Ph.D. degree in electric power and power electronics program with Texas A&M University, College Station, TX, USA, in 2010.

He was with LG electronics, Seoul, from 2006 to 2007. He was a Research Engineer with Toshiba International Corp., Houston, TX, USA, from 2009 to 2012. He has been an Assistant Professor with the University of Akron, Akron, OH, USA, from 2012. His current research interests include the degradation modeling, fault tolerant control, and fault tolerant design of electric machine and power electronics system.



Md Zakirul Islam (S'15) received the B.Sc. degree in electrical and electronic engineering from the Bangladesh University of Engineering and Technology, Dhaka, Bangladesh, in 2009. He is currently pursuing the Ph.D. degree with the University of Akron, Akron, OH, USA, in 2014.

He was with Robi Axiata BD Limited, Dhaka, from 2009 to 2014. He has been researching on the design and control of electrical machines with an emphasis on rare-earth-free electric machines.



Sangshin Kwak (S'02–M'05) received the Ph.D. degree in electrical engineering from Texas A&M University, College Station, TX, USA, in 2005.

From 2007 to 2010, he was an Assistant Professor with Daegu University, Gyeongsan, South Korea. Since 2010, he has been with Chung-Ang University, Seoul, South Korea, where he is currently an Associate Professor. His current research interests include topology design, modeling, control, and analysis of power converters including resonant converters for adjustable speed drives and digital display drivers as well as modern control theory applied to DSP-based power electronics.



Jeihoon Baek (S'03–M'10) received the M.S. degree in electrical engineering from the University of Wisconsin–Madison, Madison, WI, USA, in 2006, and the Ph.D. degree in electrical engineering from Texas A&M University, College Station, TX, USA, in 2009.

From 1998 to 2000, he was with Amotech, Seoul. He was a Senior Research Engineer with Samsung Electromechanics, Suwon, South Korea, from 2000 to 2003. From 2010 to 2013, he was a Principal Engineer with the Samsung Advanced Institute of Technology, Youngin, South Korea. Since 2014, he has been with the Korea Railroad Research Institute, Uiwang, South Korea. His current research interests include the design and analysis of electrical machines, variable speed drives for traction and propulsion applications, and novel power conversion topology.